Primljen / Received: 31.10.2014.
Ispravljen / Corrected: 21.1.2015.
Prihvaćen / Accepted: 19.3.2015.
Dostupno online / Available online: 1.8.2015.

Numerical evaluation of structural wall – flat slab connection

Authors:

Surumi Rasia Salim, MCE
Anna University Chennai
Faculty of Civil Engineering
India
surumirazia@gmail.com

Prof. Krishnan Prabhakan Jaya
Anna University Chennai
Faculty of Civil Engineering
India
jayakp@annauniv.edu

Assist.Prof. Greeshma Sivasankarapillai
Anna University Chennai
Faculty of Civil Engineering
India
greeshmas@annauniv.edu

Scientific paper - Subject review

Surumi Rasia Salim, Krishnan Prabhakan Jaya, Greeshma Sivasankarapillai

Numerical evaluation of structural wall – flat slab connection

The response of the exterior shear wall to flat slab connection, subjected to the in-plane reversible cyclic load, is analyzed in the paper. The numerical analysis of the exterior wall-slab connection specimens scaled down to one third of the original size, with two types of joint detailing patterns, was conducted. The conventional pattern and a proposed nonconventional joint reinforcement detailing pattern were considered. It was established that the performance of the proposed nonconventional type of joint detailing is better compared to that of the conventional type.

Key words:
reinforced concrete, shear wall – flat slab connection, finite element method, nonlinear analysis

Pregledni rad

Surumi Rasia Salim, Krishnan Prabhakan Jaya, Greeshma Sivasankarapillai

Numerička ocjena spoja nosivog zida i ravne ploče

U radu je provedena analiza odziva spoja vanjskog posmičnog zida i ravne ploče za slučaj ravninskog reverzibilnog cikličnog opterećenja. Provedena je numerička analiza spoja vanjskog zida i ploče na uzorcima umanjenima na jednu trećinu od prvobitne veličine, uz primjenu dviju vrsta rasporeda armature u spoju. Razmatran je konvencionalan raspored i predloženi nekonvencionalan raspored razrade armature spoja. Ustanovljeno je da se predloženi nekonvencionalni tip armiranja spoja bolje ponaša od konvencionalnog tipa.

Ključne riječi:
armirani beton, spoj posmičnog zida i ravne ploče, metoda konačnih elemenata, nelinearna analiza

Übersichtsarbeit

Surumi Rasia Salim, Krishnan Prabhakan Jaya, Greeshma Sivasankarapillai

Numerische Beurteilung der Verbindung zwischen Tragwand und Flachdecke

In dieser Arbeit ist das Verhalten der Verbindung von äußerer Wandscheibe und Flachdecke bei wechselseitiger zyklischer Belastung in der Ebene analysiert. Numerische Analysen der Verbindung zwischen Außenwand und Platte sind für Proben im Maßstab 1:3 durchgeführt, unter Berücksichtigung zwei verschiedener Verbindungsdetails. Dabei wurden eine herkömmliche und eine vorgeschlagene unkonventionelle Bewehrungsanordnung für die Verbindung erfragt. Bei dem vorgeschlagenen unkonventionellen Detail ist ein besseres Verhalten als bei dem herkömmlichen Detail festgestellt worden.

Schlüsselwörter:
Stahlbeton, Verbindung Wandscheibe-Flachdecke, nichtlineare Analyse

1. Introduction

The study of the behaviour of connections is of paramount importance for understanding the seismic resistance of structures. The analysis of such behaviour calls for modelling of materials, modelling of the structure, and load modelling. The finite-element analysis will probably be the best choice to incorporate variances in the above parameters. Several attempts have been made so far to model and analyse reinforced-concrete structural elements and joints. However, due to considerable advancement in the field of computational mechanics, the efficiency of prominent software programs to predict the response of structures has already been confirmed [1-6].

In the past decade, various studies were undertaken to address the lack of information on the interaction between the floor slabs and shear walls [7-10]. The design procedure for shear walls is considered in major international codes such as the ACI, Eurocode, Canadian, New Zealand, and British codes, code of the Architectural Institute of Japan, etc. However, the detailing of the shear wall–floor slab connection has been mentioned in BS Eurocodes only [11, 12]. Hence, an attempt has been made to analyse behaviour of the connection with the conventional detailing as per British Standards [12], and a proposed non - conventional detailing option, in order to enable an integral and better performance of the structural system. The detailing of the wall to slab connection subassemblies is expected to address the joint shear, confinement of concrete, proper construction ability, and proper provision of anchorage. Although the provision of additional horizontal U hooks connecting the shear wall and slab, as per British Standards [12], meets the expectations, the void joint core is identified as the part to be modified. To this purpose, stirrups are being proposed in the joint core connecting consecutive U hooks.

2. Development of wall-slab connection specimens

2.1. Analysis and design of prototype structure

An eight storey reinforced concrete building located in Chennai, India (in seismic zone III as per IS 1893 (Part 1): 2002) [13] on medium-quality soil, was analysed. The storey height of 3.5 m was adopted for all levels. The slab measuring 4 m x 2.5 m x 0.25 m was connected to the shear wall 2.5 m x 0.3 m in cross section. The plan and elevation of the building are shown in Figure 1. The longitudinal and transverse beams measured 500 mm in depth and 200 mm in width. The live load of 2 kN/m^2, and floor finish of 1 kN/m^2, were adopted for analysis. The C30/37 grade concrete and Fe 415 grade steel were used in the design. The seismic analysis was performed using the equivalent lateral force method recommended in IS 1893 (Part 1): 2002 [13]. The shear forces, bending moments, and axial forces around the wall - slab interface, resulting from different load combinations, were determined and the following critical design forces for the section were obtained: axial load 1903.45 kN, shear force 311.74 kN, and moment 1690.5 kNm. The design and detailing of the shear wall and slab were conducted based on the guidelines given in IS 456: 2000 [14] and IS 13920: 1993 [15], respectively.

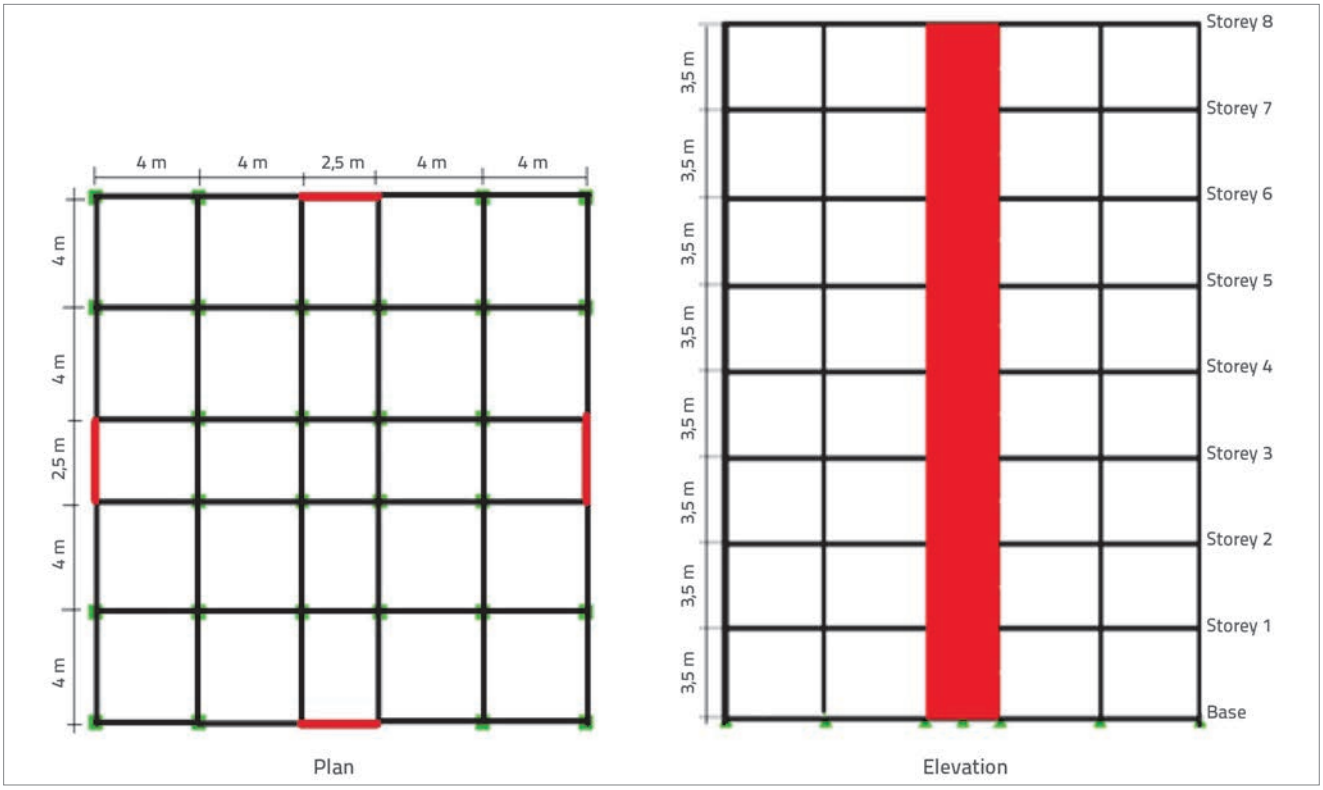

Figure 1. Details of prototype structure

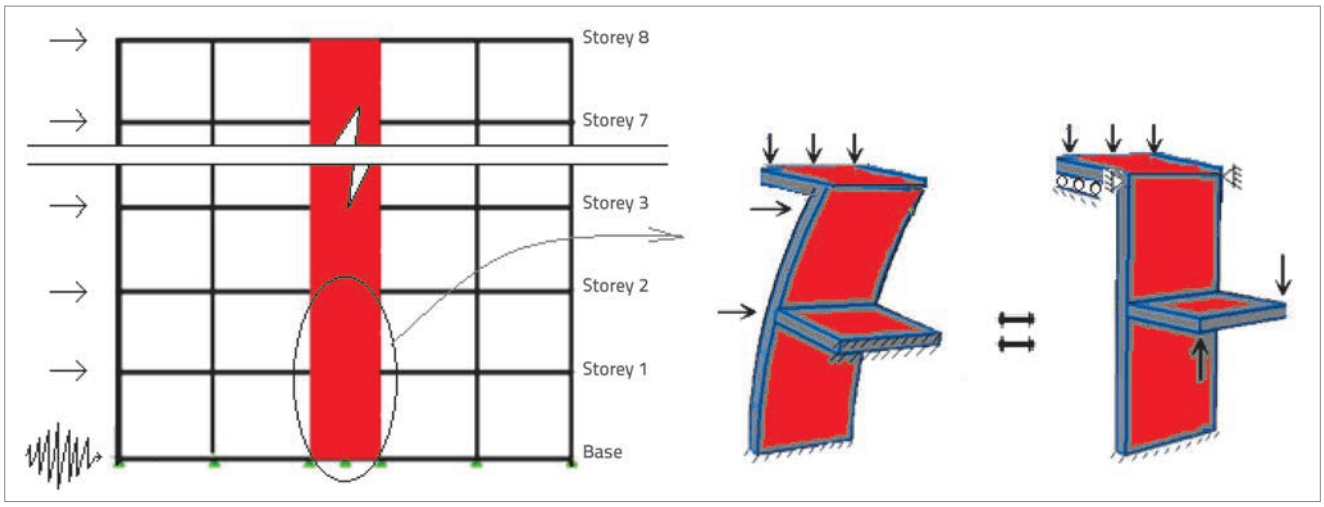

Figure 2. Exterior wall-slab connection specimen

2.2. Details of wall-slab connection specimen

The external wall-slab connection at the first storey, illustrated in Figure 2, was considered for the study. To analyse this connection, an equivalent system of forces in the slab is to be generated, which will induce the same joint effects due to the original in-plane loading of wall under earthquake action. To achieve this, the top of the shear wall is to be restrained from in-plane motion, while the out-of-plane movement due to axial load is to be allowed. The connection specimens are one-third scaled down models of the designed exterior wall-slab connection sub-assemblage. The test specimen consists of the base storey shear wall, a portion of the first floor slab, and the first storey shear wall. The top slab is also considered for application of axial load onto the specimen. The geometry of the connection specimens is shown in Figure 3 and Figure 4.

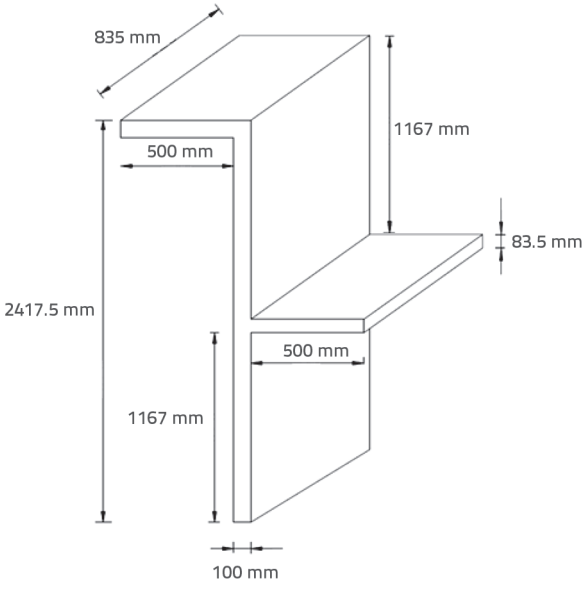

Figure 3. Geometry of connection sub-assembly

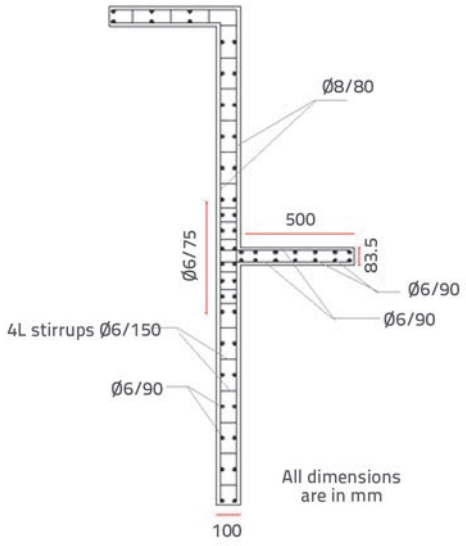

Figure 4. Specimen reinforcement details

2.3. Types of wall-slab connections

Two types of connections with different joint detailing options were considered for the study. These two joint detailing types are represented in Figure 5. They were designated as Type 1 and Type 2 based on the type of detailing.

Type 1 - Conventional detailing: The wall-slab connection is detailed in conventional manner with the provision of hooks connecting the shear wall and floor slab. The hooks were extended into the slab to a length equal to the development length of the reinforcement.

Type 2 – Nonconventional detailing: The wall-slab connection is detailed with extra stirrups provided throughout the joint core connecting the consecutive hooks.

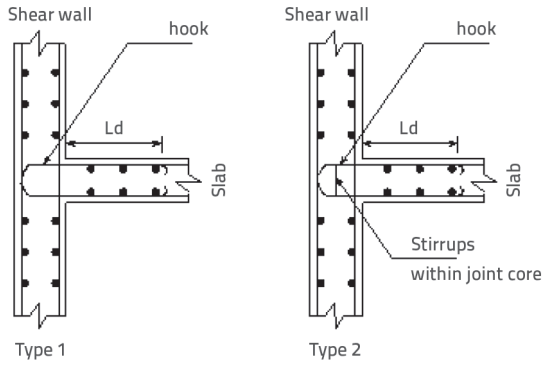

Figure 5. Types of connection

3. Development of finite element model

Reinforced concrete structures are widely employed in engineering practice for a variety of situations and applications. While traditional methods remain adequate for the analysis and design of reinforced concrete members, the development of the finite-element method has provided means for the analysis of much more complex systems in a more realistic way. The main obstacle to the finite-element analysis of reinforced concrete structures is the difficulty in the characterisation of material properties. Much effort has been spent in the search of a realistic model to predict behaviour of reinforced concrete structures. Due to complex composite nature of the material, proper modelling of such structures is considered to be a highly challenging task. ABAQUS/CAE [16] can provide solutions for the linear, non-linear and explicit problems. Its powerful graphic interface allows an accurate definition of the model, and is particularly useful for the visualisation and presentation of analytical results.

3.1. Element types

3.1.1. Concrete

ABAQUS provides two models for the non-linear concrete behaviour viz. Concrete Smeared Cracking and Concrete Damage Plasticity (CDP) model. Smeared cracking is used for simple structures subjected to monotonic loading. It is based on the damaged elasticity formulation and consists in the detection of a number of micro cracks, including their propagation. Concrete damaged plasticity is mainly used for structures subjected to cyclic and dynamic loading. The most significant difference between the damaged plasticity and smeared cracking is the ability to define compression and tension degradation. The damage property lowers the elastic stiffness when the element plasticizes. Therefore, it cannot recover its initial strength, which is especially important for cyclic loading. The range of degradation is defined by the user.

The concrete element behaviour under cyclic loading is represented with curves given in Figure 6. The element is subjected to tension exceeding the tensile strength. The cracking causes partial damage of the material, which can be defined by the parameter d_t and, when the element is unloaded, the modulus of elasticity changes to $(1-d_t)E_0$. If the element is compressed afterwards, its elastic behaviour is determined by the parameter w_c and the elasticity modulus in compression is defined as $(1-d_t+w_c d_t)E_0$. Assuming that cracks do not influence the stiffness in compression, the parameter w_c is to be defined as 1.

When the value of the parameter w_c equals zero (full degradation), the stiffness in compression is identical to the tension stiffness. The crushed section loses its initial properties in compression, defined by the parameter d_c, and initial properties in tension, defined by the parameter d_t.

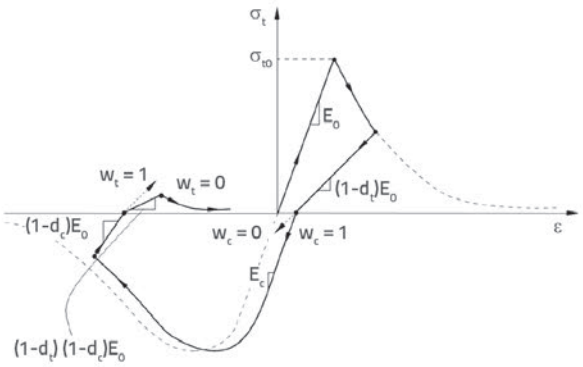

Figure 6. Concrete damage plasticity model under cyclic loading

Concrete damage plasticity parameters are to be divided into three groups in the material property window viz. Compressive Behaviour, Tensile Behaviour, and Plasticity. The compression hardening data input in terms of crushing strain for C30/37 grade concrete is provided in Table 1, and the unloading data in terms of tensile damage are given in Table 2.

The tension stiffening data input in terms of cracking strain for C30/37 grade concrete is presented in Table 3, and the unloading data in terms of tensile damage are given in Table 4.

Table 1. Concrete compression hardening

Yield stress [MPa]	Crushing strain
13	0
20	0.0007
24	0.001
37.5	0.002
22.5	0.0035
16	0.05

Table 2. Concrete compression damage

Damage parameter d_c	Inelastic strain
0	0
0	7.47E-05
0	9.89E-05
0	0.0001541
0	0.0007615
0.195402	0.0025576
0.596382	0.0056754
0.894865	0.0117331

Table 3. Concrete tension stiffening

Yield stress [MPa]	**Cracking strain**
3.5	0
1.75	0.00015
0.8	0.00035
0.25	0.0006

Table 4. Concrete tension damage

Damage parameter d_t	Cracking strain
0	0
0	3.33E-05
0.406411	0.0001604
0.69638	0.0002798

Elasticity and plasticity parameters are required in addition to the hardening and stiffening variables to define the yield function for the CDP model. The various CDP input parameters are given in Table 5.

Table 5. CDP model parameters

CDP parameters	Input values
Poisson's Ratio	0.2
Young's Modulus (E)	27386.127 N/mm^2
Dilation Angle (φ)	38°
Initial Biaxial / Uniaxial ratio	1.16
Ratio of second stress invariant on tensile meridian (Kc)	0.67
Viscosity parameter	0
Flow potential eccentricity (ε)	0.1

3.1.2. Steel

The steel reinforcement is modelled as an elastoplastic material. The stress-strain characteristics of the reinforcing steel bars are shown in Figure 7. In tension, it exhibits an initial linear elastic portion, $\sigma_s = E_s \cdot \varepsilon_s$, which is followed by a yield plateau at $\sigma_s = f_y$, beyond which the strain increases with little or no change in stress, and the strain-hardening range until rupture occurs at the tensile strength, $\sigma_s = f_{su}$. The input data for the reinforcing steel grade F 415 is given in Table 6.

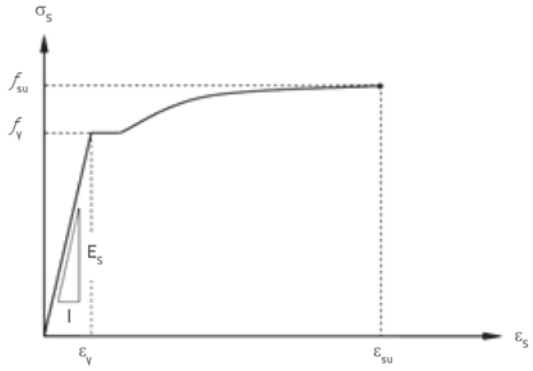

Figure 7. Stress - strain characteristics of steel

Table 6. Steel model parameters

Elasticity	
Young's Modulus [MPa]	**Poisson's Ratio**
20000	0,3
Plasticity	
Yield stress [MPa]	**Plastic strain**
413.69	0
415	0.00207
416	0.0205
450	0.0478
485	0.12
300	0.1292
100	0.139

3.2. Modelling of connection specimens

In this study, 3D deformable solid extrusion elements were used for modelling the concrete part. 3D deformable wire planar elements were used for modelling the reinforcing steel parts. Rebars were assigned with beam sections with circular profile of required diameter. The modelling of the two joint specimens with different types of detailing was done using the element types and material properties as discussed above. The reinforcement configuration in the model is shown in Figure 8. The wall reinforcement was modelled discretely and meshed using a 2-node beam element (B31). The assigned homogenous solid concrete section was meshed using hexagonal 8-node brick elements (C3D8R). Full bond between the concrete and reinforcement was assumed using the embedded region constraint interaction between steel and concrete sections. The embedded constraint is presented in Figure 9. The meshing details are given in Table 7.

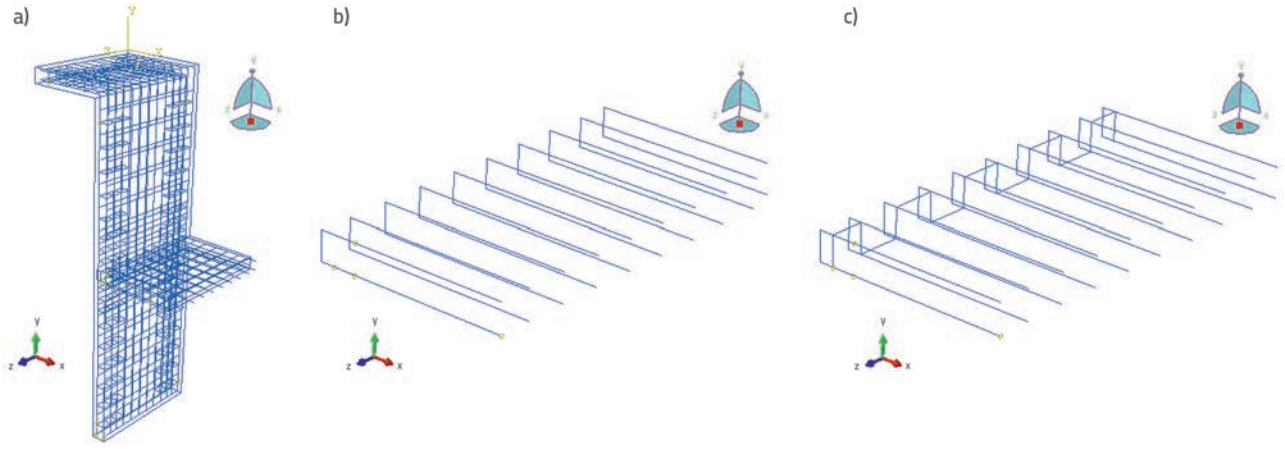

Figure 8. Connection specimen models: a) subassembly model; b) type 1 joint modelling; c) type 2 joint modelling

Table 7. Details of meshing

Mesh module	Concrete	Rebar
Element type	C3D8R: An 8-node linear brick, hexagonal	B31: A 2-node linear beam in space
Family	three dimensional stress	beam
Global seed size	40	20
Finite element	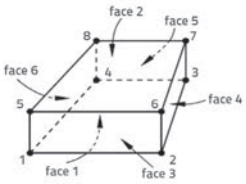	
Element s mrežom	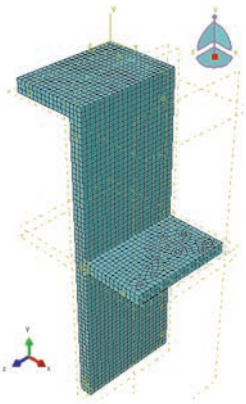	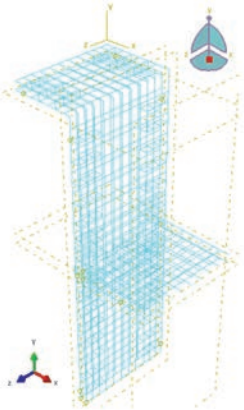

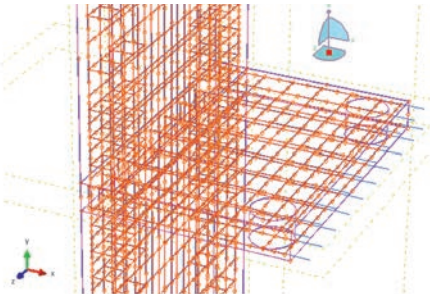

Figure 9. Embedded region constraint interaction

3.3. Boundary conditions and loading protocol

The shear wall is assumed to be fixed at the base. For this, all degrees of freedom are constrained at the shear wall base. At the top of the shear wall, the in-plane motion is restrained while the out-of-plane movement due to axial load is allowed. The axial load and the out-of-plane moment at the top of the subassembly was distributed as pressure at the top slab of the specimen. The loading and boundary conditions of the specimen are shown in Figure 10. The displacement controlled loading was achieved by

defining partitions of circular profile and by assigning a prescribed displacement to the partitions. The scheduled loading protocol shown in Figure 11 was assigned to the circular partitions. The prescribed displacement cycles were achieved using the smooth step amplitude function. The cyclic loading amplitude was increased in 0.5 mm increments, with three cycles of each displacement amplitude level, until failure of the specimen.

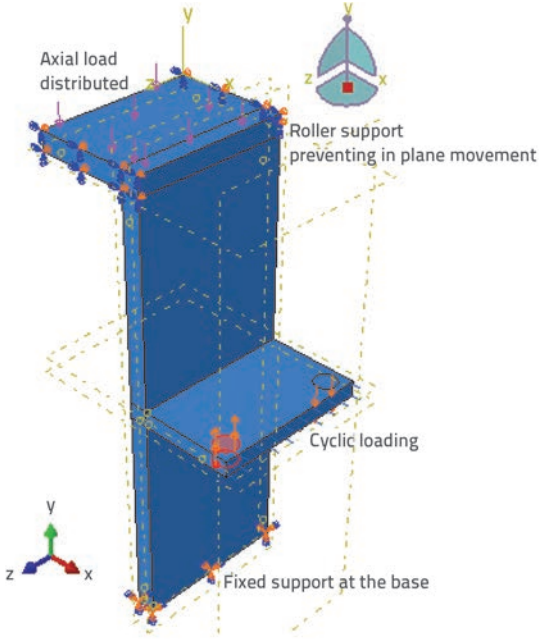

Figure 10. Loading and boundary conditions of connection subassembly

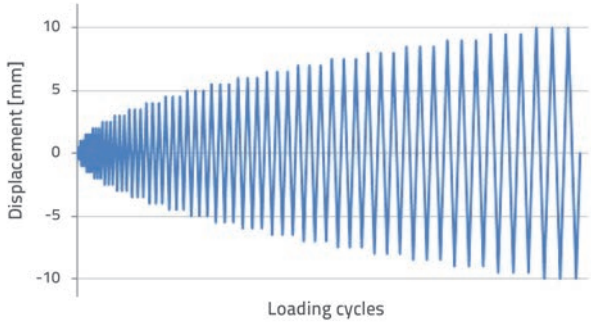

Figure 11. Sequence of loading

4. Results and discussion

4.1. Strength

The comparison of strength of the two types of connection specimens in the positive and negative directions is given in Figure 12. The specimen with the type 2 detailing performed better than the type 1 specimen. The type 2 specimen exhibited the load carrying capacity that is by 31.7 % and 30.9 % greater than that of the conventional type 1 specimen in the positive and negative directions, respectively.

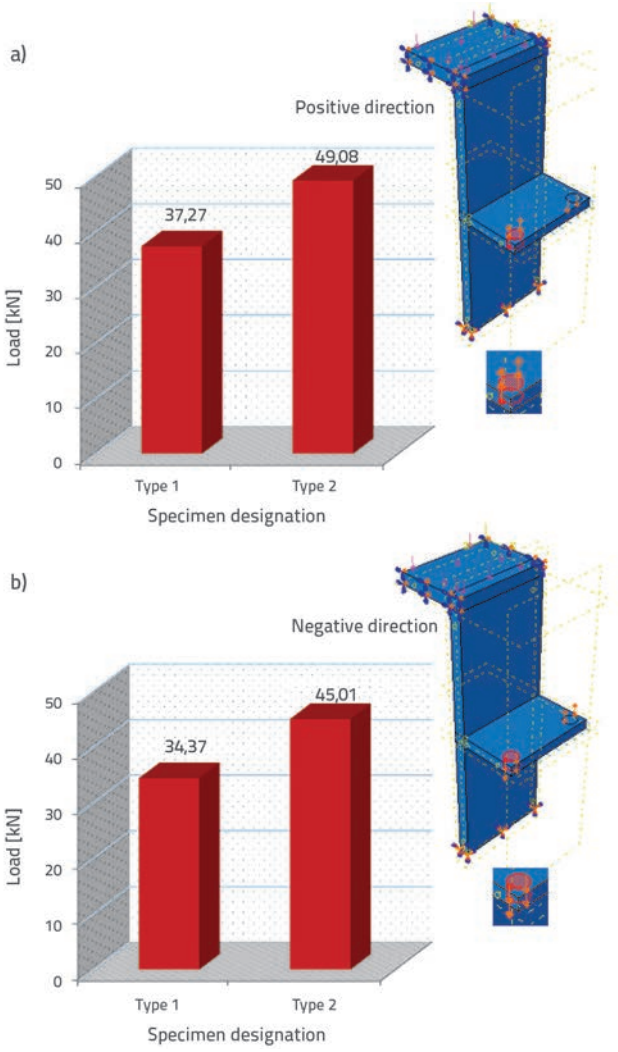

Figure 12. Specimen strength comparison: a) positive direction; b) negative direction

4.2. Load-displacement behaviour

The load-displacement behaviour for the cyclic loading at each displacement excursion level of the two types of specimens is shown in Figure 13. The specimens exhibited fat hysteresis loops with a very low pinching, due to good bonding between the reinforcement and joint concrete. Since bar slipping was not taken into account, the model could not reflect the pinching characteristics. Although ABAQUS can estimate the capacity and behaviour of connection specimens quite well, it can not accurately account for pinching effects on cyclic behaviour of reinforced concrete elements [17]. This feature was initially suggested by Wan et. al [18]. The curves showed similar performance in stiffness and strength degradation during displacement cycles. It was established that the stirrups within the joint core region participated in the resistance, and increased the capacity of the joint.

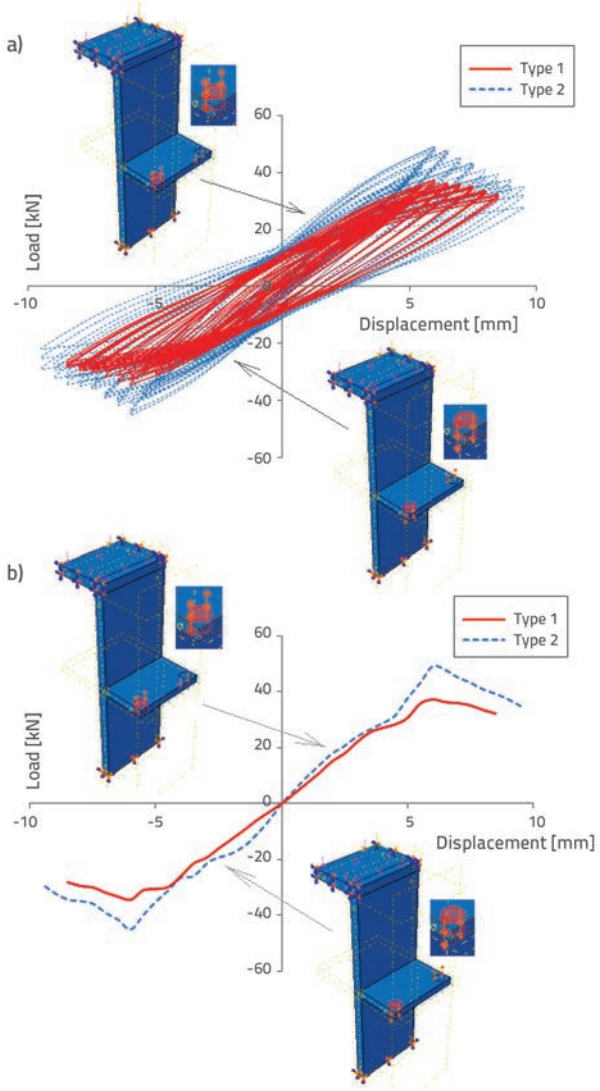

Figure 13. Load-displacement behaviour: a) hysteresis loops; b) envelope

4.3. Ductility and energy dissipation capacity

The ductility measured in terms of displacement ductility, calculated as per ASCE guidelines [19], is presented in Table 8. It was established that the displacement ductility is by 42.7 % greater for the type 2 specimen compared to the type 1 specimen. A connection subjected to cyclic loading is considered to be ductile if a sufficient amount of energy is dissipated without a substantial loss of strength and stiffness. The area enclosed by the hysteretic loop in a given cycle represents the energy dissipated by that specimen during that cycle. The cumulative energy dissipated was computed by summing up the energy dissipated in consecutive cycles throughout the test. The comparison of energy dissipated during each cycle of loading, plotted against the corresponding displacement cycle for the specimens, is shown in Figure 14. The 81.15 % increase was found in the cumulative energy dissipation capacity for the type 2 specimen, when compared to that of the conventional specimen.

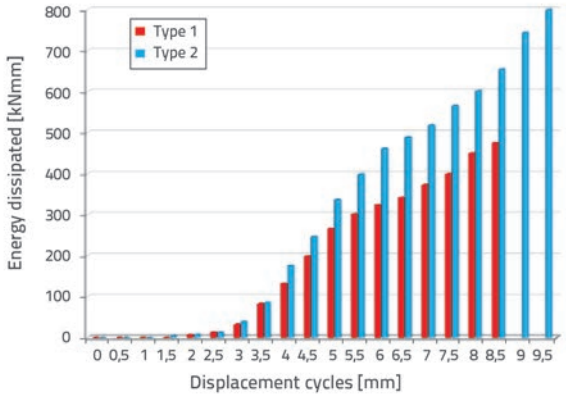

Figure 14. Comparison of energy dissipation capacity

4.4. Joint stress

The comparison of the Von Mises stress in the joint bars is shown in Figure 15. An increased stress level was observed in the Type 2 specimen due to the effect of stirrups in the core, and it is resisted within the joint. It was established that the hooks of the conventionally detailed specimen at the joint region were stressed to some extent, and that it thus developed damage at the slab and shear wall interface. In the Type 2 specimen, the stirrups confined the joint core thus ensuring a uniform distribution of stresses in the vertical element bars.

The stirrups in the core region could take care of the joint shear demands by arresting the tensile forces (45^0) due to shear, as shown in Figure 16. The stirrups would also provide an increased confinement of the joint core region. The effect of such concrete core confinement, increased shear assuming capacity, and better anchorage, resulted in a higher overall capacity of the connection.

Table 8. Comparison of displacement ductility of specimens

Specimen	Yield displacement Δ_y [mm]		Ultimate displacement Δ_u [mm]		Displacement ductility factor μ		Average displacement ductility factor μ
	Positive	Negative	Positive	Negative	Positive	Negative	
Type 1	3.00	2.49	5.03	4.48	1.67	1.79	1.73
Type 2	3.10	2.53	7.18	6.66	2.31	2.63	2.47

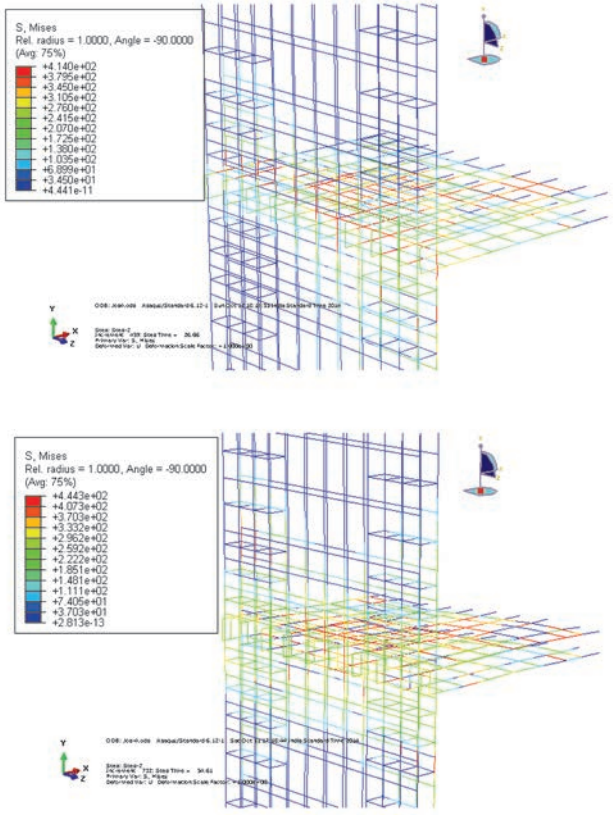

Figure 15. Von mises stress at the joint:a) type 1 specimen; b) type 2 specimen

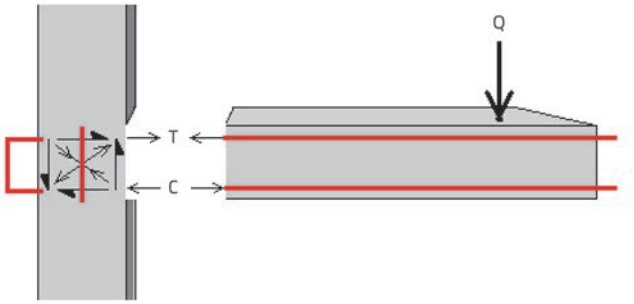

Figure 16. System of forces at joint

5. Conclusion

In this paper, a numerical study was made to determine the effectiveness of a proposed joint reinforcement detailing pattern for the exterior wall to slab connection subjected to cyclic loading. The results obtained show that the specimen with the proposed joint detailing with stirrups in the core region exhibited a higher ultimate strength compared to a conventional specimen. The maximum average ultimate strength of the Type 2 specimens is by 31.3 % higher than that of the type 1 specimens. For both specimens, the spindle-shaped hysteretic loops were observed with a large energy dissipation capacity. An increase of 81.15 % in the cumulative energy dissipation capacity was established for the Type 2 specimen when compared to that of the conventional specimen. The enhancement in deformation capacity of the Type 2 specimen was by 42.7 % greater when compared to the Type 1 specimen. This behaviour of the proposed detailing type satisfies fundamental requirements of seismic resistance such as the ductility and energy dissipation capacity. Considering the performance of the connections, it can be concluded that the provision of stirrups within the joint core region can be an effective option for detailing the exterior shear wall – flat slab connection in seismic prone areas.

Acknowledgement

The financial assistance provided by Anna University, Chennai, through the Anna Centenary Research Fellowship grant, is greatly acknowledged by the authors.

REFERENCES

[1] Fanning, P.: Nonlinear Models of Reinforced and Post-tensioned Concrete Beams, Electronic Journal of Structural Engineering, 2 (2001), pp. 111-119.

[2] Hidalgo, P.A., Jordan, R.M., Martinez, M.P.: An analytical model to predict the inelastic seismic behavior of shear-wall, reinforced concrete structures, Engineering Structures, 24 (2002) 1, pp. 85-98.

[3] Coull, A., Chee, W.: Effect of Local Elastic Wall Deformations on the Interaction between Floor Slabs and Flanged Shear Walls, Journal of Structural Engineering, ASCE 110 (1983) 1, pp. 105-119.

[4] Coull, A., Chee, W.: Stiffening of Structural Cores by Floor Slabs, Journal of Structural Engineering, ASCE, 112 (1986) 5, pp. 977-994.

[5] Bari, M.: Non linear finite element study of shear wall floor slab connection, Journal of Civil Engineering, The institution of engineers, Bangladesh CE 24 (1996) 2, pp. 137-145.

[6] Uma, S.R., Meher Prasad, A.: Seismic behaviour of beam-column joints in RC moment resisting frames: A review, Indian Concrete Journal, Vol.80 (2006) 1, pp. 33-42.

[7] Siti, I., Yee, H., M.: An Investigation on effect of Rebar on Structural behaviour for wall-slab system, IEEE Business, Engineering & Industrial applications Colloquium (BEIAC), (2012), No.978-1-4673-0426-9/12, pp. 26-29.

[8] Al-aghbari, A., Hamid, N., Rahman, N., Hamzah, S.: Structural Performance of two types of wall slab connection under out-of-plane lateral cyclic loading, Journal of Engineering science and technology, 7 (2012) 2, pp. 177-194.

[9] Greeshma, S., Jaya, K.P.: Effect of Cross inclined bars on the behaviour of shear wall-floor slab joint under lateral cyclic loading, Journal of Structural Engineering (2012), Special Issue, April, Ref. No. 320(28/B)/2012/JOSE.

[10] Greeshma, S., Jaya, K.P., Rajesh, C.: Seismic Behaviour of Shear Wall – Slab Joint under Lateral Cyclic Loading, Asian Journal of Civil Engineering (Building and housing), 13 (2012) 4, pp. 455-464.

[11] BS EN 1992-1-1: Eurocode 2: Design of Concrete Structures - Part 1-1:General rules and rules for buildings, 2004.

[12] BS EN 1998-1: Eurocode 8: Design of Structures for Earthquake Resistance - Part 1:General Rules, seismic actions and rules for buildings, 2004.

[13] IS 1893 (Part 1): Indian Standard Criteria for earthquake resistant design of structures, Bureau of Indian Standards, New Delhi, India, 2002.

[14] IS 456: Indian Standard Plain and Reinforced Concrete Code of Practice, Bureau of Indian Standards, New Delhi, India, 2000.

[15] IS 13920: Indian Standard Ductile Detailing of Reinforced Concrete Structures subjected to Seismic forces, Bureau of Indian Standards, New Delhi, India, 1993.

[16] Abaqus 6.12: Abaqus/CAE user's manual version, Dassault Systèmes, Dassault Systèmes Simulia Corp., Providence, RI, USA, 2012.

[17] Mousavi, S.A., Zahrai, S.M., Bahrami-Rad, A.: Quasi-static cyclic tests on super-lightweight EPS concrete shear walls, Engineering Structures, 64 (2014), pp. 62-75, http://dx.doi.org/10.1016/j.engstruct.2014.02.003

[18] Wan, S., Loh, C.H., Peng, S.Y.: Experimental and theoretical study on softening and pinching effects of bridge column, Soil Dynamics and Earthquake Engineering, 21 (2001), pp. 75-81, http://dx.doi.org/10.1016/S0267-7261(00)00073-7

[19] ASCE: State-of-the-art report on finite element analysis of reinforced concrete, New York, 1982.